



Cancer Research

Blockade of Mitogen-Activated Protein Kinase/Extracellular Signal-Regulated Kinase Kinase and Murine Double Minute Synergistically Induces Apoptosis in Acute Myeloid Leukemia via BH3-Only Proteins Puma and Bim

Weiguo Zhang, Marina Konopleva, Jared K. Burks, et al.

Cancer Res 2010;70:2424-2434. Published OnlineFirst March 9, 2010.

Updated Version

Access the most recent version of this article at:
doi:[10.1158/0008-5472.CAN-09-0878](https://doi.org/10.1158/0008-5472.CAN-09-0878)

Supplementary Material

Access the most recent supplemental material at:
<http://cancerres.aacrjournals.org/content/suppl/2010/03/08/0008-5472.CAN-09-0878.DC1.html>

Cited Articles

This article cites 51 articles, 23 of which you can access for free at:
<http://cancerres.aacrjournals.org/content/70/6/2424.full.html#ref-list-1>

Citing Articles

This article has been cited by 1 HighWire-hosted articles. Access the articles at:
<http://cancerres.aacrjournals.org/content/70/6/2424.full.html#related-urls>

E-mail alerts

[Sign up to receive free email-alerts](#) related to this article or journal.

Reprints and Subscriptions

To order reprints of this article or to subscribe to the journal, contact the AACR Publications Department at pubs@aacr.org.

Permissions

To request permission to re-use all or part of this article, contact the AACR Publications Department at permissions@aacr.org.

Blockade of Mitogen-Activated Protein Kinase/Extracellular Signal-Regulated Kinase Kinase and Murine Double Minute Synergistically Induces Apoptosis in Acute Myeloid Leukemia via BH3-Only Proteins Puma and Bim

Weiguo Zhang¹, Marina Konopleva^{1,2}, Jared K. Burks¹, Karen C. Dywer¹, Wendy D. Schober¹, Jer-Yen Yang^{3,4,5}, Teresa J. McQueen¹, Mien-Chie Hung^{3,5}, and Michael Andreeff^{1,2}

Abstract

Molecular aberrations of the Ras/Raf/mitogen-activated protein kinase/extracellular signal-regulated kinase (ERK) kinase (MEK)/ERK and/or Murine double minute (MDM2)/p53 signaling pathways have been reported in 80% and 50% of primary acute myeloid leukemia (AML) samples and confer poor outcome. In this study, antileukemic effects of combined MEK inhibition by AZD6244 and nongenotoxic p53 activation by MDM2 antagonist Nutlin-3a were investigated. Simultaneous blockade of MEK and MDM2 signaling by AZD6244 and Nutlin-3a triggered synergistic proapoptotic responses in AML cell lines [combination index (CI) = 0.06 ± 0.03 and 0.43 ± 0.03 in OCI/AML3 and MOLM13 cells, respectively] and in primary AML cells (CI = 0.52 ± 0.01). Mechanistically, the combination upregulated levels of BH3-only proteins Puma and Bim, in part via transcriptional upregulation of the FOXO3a transcription factor. Suppression of Puma and Bim by short interfering RNA rescued OCI/AML3 cells from AZD/Nutlin-induced apoptosis. These results strongly indicate the therapeutic potential of combined MEK/MDM2 blockade in AML and implicate Puma and Bim as major regulators of AML cell survival. *Cancer Res*; 70(6); 2424–34. ©2010 AACR.

Introduction

Acute myeloid leukemias (AML) are clonal malignancies of the hematopoietic stem cell. Many aberrant molecular events have been implicated in leukemogenesis. For example, constitutive activation of the mitogen-activated protein kinase (MAPK) signaling pathway is reported in >80% of primary AML samples (1) and was identified by us as an independent prognostic factor in patients with AML (2). Furthermore, overexpression of the Murine double minute (MDM2) protein is present in 50% of AML (3). MDM2 not only rapidly degrades p53 through its E3 ubiquitin ligase activity (4) but is also upregulated by p53 at the transcriptional level as a

negative feedback loop of p53 activity (5). Interestingly, simultaneous loss-of-function p53 and MAPK (Ras) activation was shown to be synergistic in the malignant transformation of murine and human colon cells, and the overexpression of antiapoptotic Bcl-2 with concomitant activation of MAPK (Ras) signaling induces AML in mice (6–8).

Targeting special signaling pathways with small molecule inhibitors is a potential novel therapeutic strategy for AML. Several small molecule inhibitors of Raf/MAPK/extracellular signal-regulated kinase (ERK) kinase (MEK)/ERK signaling pathway, including CI-1040, PD98059, sorafenib, and U0126, were characterized by us and others in AML models (IC₅₀, between 0.03 and 5.4 μmol/L), but as single agents, they thus far showed only modest efficacy in clinical trials (9–13). Recently, a second-generation highly selective allosteric inhibitor of MEK1/2, AZD6244 (AstraZeneca, also known as ARRY-142886), was reported to inhibit basal phosphorylation of ERK in a series of human tumor cell lines, with an IC₅₀ of around 10 nmol/L. Based on its reported antitumor efficacy in solid tumor models of hepatocellular, colon, myeloma, thyroid, and cutaneous cancer, AZD6244 has recently entered clinical trials (14–19).⁶ Our study in human leukemic cell lines has shown that AZD6244 suppressed retinoblastoma phosphorylation and modulated cell cycle-related

Authors' Affiliations: ¹Section of Molecular Hematology and Therapy, Department of Stem Cell Transplantation and Cellular Therapy, ²Department of Leukemia, and ³Department of Molecular and Cellular Oncology, The University of Texas M.D. Anderson Cancer Center; ⁴The University of Texas Graduate School of Biomedical Sciences at Houston, Houston, Texas and ⁵Center for Molecular Medicine and Graduate Institute of Cancer Biology, China Medical University and Hospital, Taichung, Taiwan

Note: Supplementary data for this article are available at Cancer Research Online (<http://cancerres.aacrjournals.org/>).

Corresponding Author: Michael Andreeff, Section of Molecular Hematology and Therapy, Department of Stem Cell Transplantation and Cellular Therapy, Unit 448, The University of Texas M.D. Anderson Cancer Center, 1515 Holcombe Boulevard, Houston, TX 77030-4009. Phone: 713-792-7260; Fax: 713-794-4747; E-mail: mandreeff@mdanderson.org.

doi: 10.1158/0008-5472.CAN-09-0878

©2010 American Association for Cancer Research.

⁶ Clinical Trials (2007), <http://www.clinicaltrials.gov>.2008; accessed April 6, 2008.

proteins, which resulted in G₁ cell cycle arrest in AML cells with constitutively activated ERK (20).

However, similar to other MAPK inhibitors, AZD6244, as a single agent, functions as a cytostatic rather than cytotoxic agent in malignancies (20, 21). Hence, combination therapeutic strategies that target multiple signaling pathways might enhance its proapoptotic potential. For example, a small molecule antagonist of MDM2, Nutlin-3a, which induces wild-type, unmutated p53, has been shown by us to induce apoptosis in AML (22). We have recently reported that the combination of MEK inhibitor PD98059 and Nutlin-3a induces synergistic proapoptotic effects in leukemia cells (23); however, the mechanisms underlying that activity were not fully understood. In this study, we investigated the molecular mechanisms underlying antileukemic efficacy of AZD6244 and Nutlin-3a in AML.

Materials and Methods

Reagents. AZD6244 (ARRY-142886) was provided by Dr. Paul Smith, AstraZeneca, and Nutlin-3a was supplied by Dr. Lyubomir T. Vassilev, Hoffmann-La Roche. All other chemicals and solvents used were of the highest grade commercially available.

Cell lines and primary AML samples. The human AML cell lines HL60 and U937 were obtained from American Type Culture Collection, OCI/AML3 cells were kindly provided by Dr. Mark D Minden (Princess Margaret Hospital), and MOLM13 cells were obtained from Fujisaki Cell Center, Hayashibara Biochemical Laboratories, Inc. OCI/AML3-p53 short hairpin RNA (shRNA) and OCI/AML3-Vector cells were generated by retroviral infection with p53 shRNA plus green fluorescent protein (GFP) or GFP-only expressing gene, as previously described (24).

Primary peripheral blood and bone marrow samples were obtained from patients with newly diagnosed or relapsed and/or refractory AML (Supplementary Table S1). Written informed consent was obtained from each patient according to institutional guidelines.

All cells, including primary patient samples, were cultured in RPMI 1640 supplemented with 10% FCS.

Cell viability and apoptosis assays. Cell viability was assessed using the trypan blue dye exclusion method, and apoptosis was determined by Annexin V positivity detected by flow cytometry, as previously described (25). All experiments were performed in triplicate.

Western blot. For immunoblot analysis, the cells were treated with the indicated agents and then collected in lysis buffer (26). For analysis of the protein levels in different fractions of the cells, a nuclear extraction kit (Active Motif) was used for separating cytosolic and nuclear fractions following the manufacturer's instructions. The semiquantitative immunoblotting data were generated by using Scion imaging software (Beta 4.03; Scion Corporation).

TaqMan real-time reverse transcription-PCR. OCI/AML3 and MOLM13 cells were treated with indicated concentrations of AZD6244 and/or Nutlin-3a for 24 h. Total RNA was isolated, and first strand cDNA was generated using random hexamers. The mRNA expression levels of FOXO3a,

Puma, Bim, Mcl-1, and Abl-1 were quantified using TaqMan gene expression assays (Applied Biosystems), as previously described (27). The real-time PCR experiments were carried out in triplicate.

Simultaneous targeting of multiple signaling pathways. Cells were resuspended in RPMI 1640 at 3×10^5 /mL and were treated with varying concentrations of the signaling inhibitors AZD6244 and/or Nutlin-3a for 48 h. The induction of apoptosis was determined by measuring the percentage of Annexin V-positive cells with flow cytometry. The isobologram and combination index (CI) analyses were performed using CalcuSyn software (BioSoft), a widely used method for evaluating combinatorial synergy between cancer therapeutic agents (28).

Immunofluorescence staining and confocal analysis. OCI/AML3 cells were treated with AZD6244 and Nutlin-3a for 24 h. The cells were then immunostained with indicated antibodies and observed with a confocal laser scanning microscope system, as previously described (13).

Cell transfection with short interfering RNAs. For knock-down of Puma, Bim, and FOXO3a proteins, the indicated short interfering RNAs (siRNA) and mock control siRNA were purchased from Dharmacon Research, Inc. Transfections of OCI/AML3 leukemia cells were carried out by electroporation using the Nucleofection system (T-solution, X-001; Amaxa), following the manufacturer's instructions. The final concentration of siRNA was 200 nmol/L. After 24 h of transfection, the indicated concentrations of AZD6244 and Nutlin-3a were added to the cells for an additional 6 or 24 h of culturing. Apoptosis induction was determined by measuring the percentage of Annexin V-positive cells via flow cytometry, and expression level of the relative proteins was analyzed by immunoblotting.

Statistical analysis. Student's *t* test was used to analyze the immunoblot, cell growth, and apoptosis data. *P* values of <0.05 were considered statistically significant. For evaluating the synergistic efficacies of AZD6244 and Nutlin-3a, CI values were determined according to the method of Chou and Talalay (29). A CI value of 1 indicates an additive effect, a CI value of <1 indicates synergy, and a CI value of >1 indicates antagonism. The average CI values were calculated at different effect levels [50% effective concentration (EC₅₀), EC₇₅, and EC₉₀]. All statistical tests were two sided.

The details of Materials and Methods, including antibodies, cell lines, Western blot analyses, TaqMan real-time reverse transcription-PCR, immunofluorescence staining, and confocal analyses, are available online as Supplementary Data.

Results

Simultaneous targeting of MEK and MDM2 synergistically inhibits cell growth and induces apoptosis in human AML cells. We first examined the effects of the MEK inhibitor AZD6244 on cell growth and apoptosis of human AML cell lines. AML cells with constitutively activated ERK (e.g., OCI/AML3, HL60, and MOLM13 lines) were more sensitive to AZD6244-induced growth inhibition than U937 cells, which have a lower basal level of phosphorylated ERK: the

mean IC_{50} values were 0.03 $\mu\text{mol/L}$ [95% confidence interval (95% CI), 0.01–0.08 $\mu\text{mol/L}$], 0.6 $\mu\text{mol/L}$ (95% CI, 0.3–1.2 $\mu\text{mol/L}$), and 0.7 $\mu\text{mol/L}$ (95% CI, 0.5–1.0 $\mu\text{mol/L}$), respectively, compared with 40.4 $\mu\text{mol/L}$ (95% CI, 33.0–49.3 $\mu\text{mol/L}$ for U937 cells). However, only moderate apoptosis induction was observed at submicromolar concentrations (Fig. 1A).

In an effort to enhance proapoptotic effects of AZD6244 in leukemia cells, we combined MDM2 antagonist Nutlin-3a with AZD6244. Results showed synergistic apoptosis induction in p53 wild-type cells OCI/AML3 (CI = 0.06 \pm 0.03) and MOLM13 (CI = 0.43 \pm 0.03), but no significant proapoptotic effect was observed in cells with

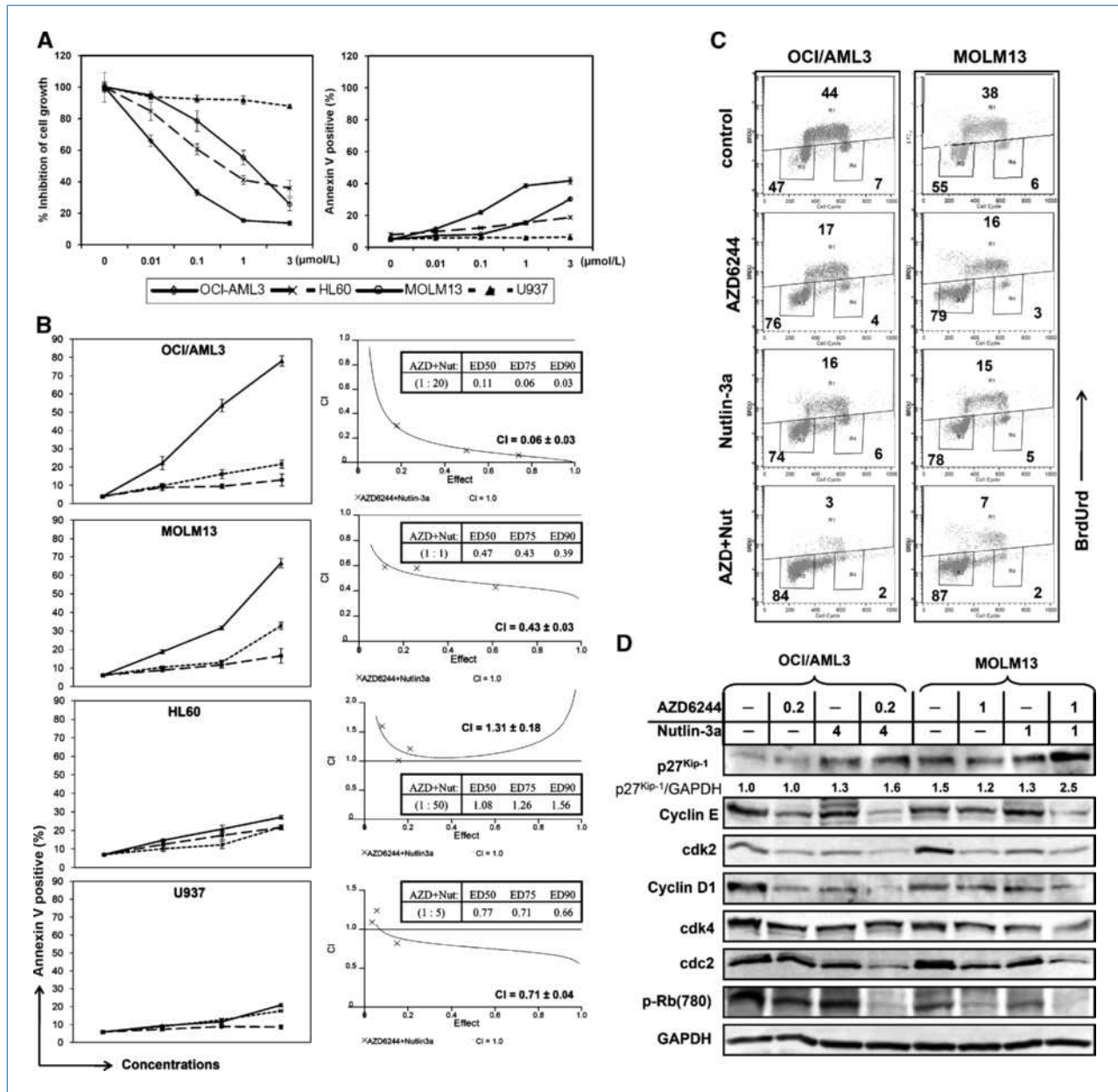


Figure 1. Combined effects of AZD6244 and Nutlin-3a on cell growth and apoptosis of human AML cell lines. **A**, OCI/AML3, MOLM13, HL60, and U937 cells were treated with indicated concentrations of AZD6244 for 72 h. Inhibition of cell growth and apoptosis were determined as described in Materials and Methods. Growth inhibition was expressed as percentage relative to that in the control group. Data represent the mean of three independent determinations. Error bars correspond to 95% CIs. **B**, OCI/AML3, MOLM13, HL60, and U937 cells were treated simultaneously with AZD6244 and Nutlin-3a using a fixed ratio as indicated, and Annexin V positivity was measured by flow cytometry after 48 h. CI values were determined by isobologram analysis. Error bars correspond to 95% CIs. **C**, OCI/AML3 and MOLM13 cells were treated with indicated concentrations of AZD6244 and/or Nutlin-3a for 24 h, after which cells were pulsed with BrdUrd for 45 min and BrdUrd incorporation was analyzed by flow cytometry following anti-BrdUrd staining. **D**, expression of cell cycle-related checkpoint proteins was determined by immunoblotting after 24 h of AZD6244/Nutlin-3a treatment.

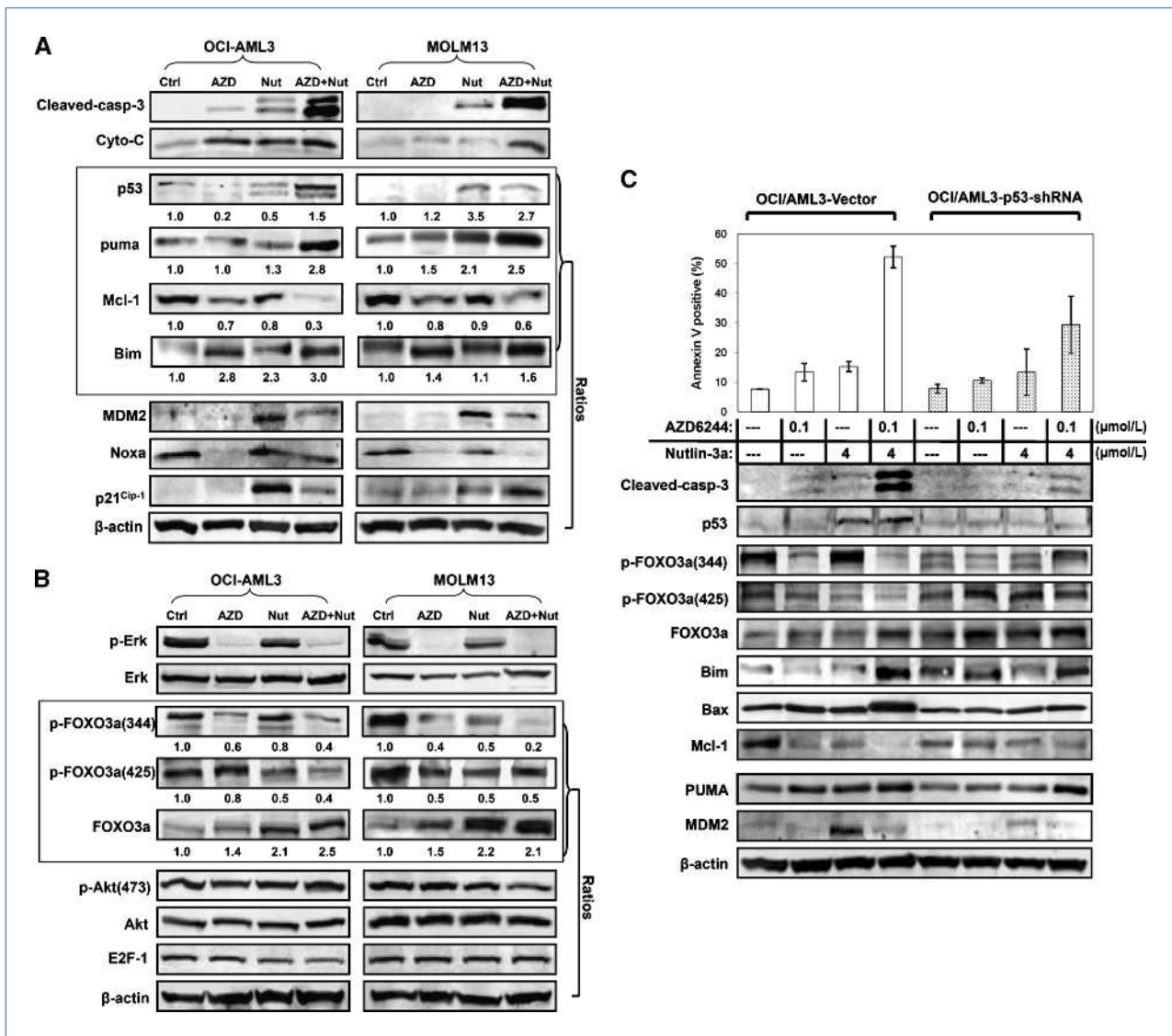


Figure 2. OCI/AML3 and MOLM13 cells were treated with AZD6244 and Nutlin-3a for 24 h. The expression of apoptosis-related proteins (A) and transcription factor FOXO3a and its downstream targets (B) were analyzed by immunoblotting. β -Actin was used as a loading control. C, OCI/AML3-Vector and OCI/AML3-p53 shRNA cells were treated at the indicated concentrations of AZD6244 and Nutlin-3a as single agents and in combination for 24 h. Apoptosis was determined as described in Materials and Methods, and the expression profiles of apoptosis-related proteins were analyzed using immunoblotting. β -Actin was used as a loading control.

dysfunctional p53 (p53-null HL-60 and p53-mutated U937; Fig. 1B).

To further investigate whether the combination treatment in the sensitive cell lines affects cell cycle progression, BrdUrd incorporation assay was determined by anti-BrdUrd staining of pulsed OCI/AML3 or MOLM13 after AZD6244 and/or Nutlin-3a treatment. Results indeed showed reduction of percentage of cells entering S phase upon combined treatment (Fig. 1C), suggesting that simultaneous targeting of MEK and MDM2 signaling inhibits cell growth by arresting cells in G_1 phase. Further investigations showed upregulation of p27^{Kip-1} and downregulation of G_1 phase-related check-

point proteins cyclin E/cyclin-dependent kinase 2 (cdk2), cyclin D1/cdk4 complexes, cdc2, and phosphorylated retinoblastoma protein in the sensitive cells OCI/AML3 and MOLM13 after combination treatment (Fig. 1D).

Combined MEK/MDM2 blockade modulates Puma, Bim, Mcl-1, and phosphorylated FOXO3a levels. To elucidate mechanisms of synergistic proapoptotic effects of the AZD6244 and Nutlin-3a combination, apoptosis-related proteins were further investigated by Western blot. Upregulation of p53, Puma (p53-upregulated modulator of apoptosis), and Bim (Bcl-2-interacting mediator of cell death) and downregulation of Mcl-1 (myeloid cell leukemia sequence 1) protein

levels were observed in cells cotreated with AZD/Nutlin, which exceeded the changes caused by either drug alone. Nutlin-3a induced MDM2 as previously reported, but this effect was blunted upon combined treatment. In turn, p21 and Noxa were modified differently in OCI/AML3 and MOLM13 cells (Fig. 2A).

We next investigated modulation of expression of the transcription factor FOXO3a, a known modulator of Bim expression. Interestingly, AZD6244, as a single agent, profoundly suppressed FOXO3a phosphorylation at the Ser³⁴⁴ and less so at the Ser⁴²⁵ site, and combined treatment further suppressed FOXO3a phosphorylation at both sites and upregulated total FOXO3a level. On the contrary, the levels of phosphorylated Akt and E2F-1 were not significantly affected by the treatment in OCI/AML3 and MOLM13 cells (Fig. 2B). To further investigate the role of p53 in the modulation of related proteins and apoptosis induction, we used p53

knockdown cells (OCI/AML3-p53 shRNA) and their respective vector-transduced cells (OCI/AML3-Vector). AZD6244 and AZD6244/Nutlin-3a blocked phosphorylated FOXO3a in p53 wild-type cells, but not in cells with silenced p53 (Fig. 2C). Notably, basal levels of total FOXO3a were higher in p53 knockdown OCI/AML3 than in p53 wild-type cells, and combination treatment upregulated total FOXO3a in a p53-independent fashion. BH3-only proapoptotic protein Bim showed a pattern similar to that of total FOXO3a. In addition, downregulation of Mcl-1 and upregulation of Bax were more significant in p53 wild-type compared with p53 knockdown OCI/AML3 cells. Likewise, apoptosis induction was higher in the p53 wild-type cells than that in the p53 knockdown cells (52% versus 29% Annexin V-positive cells). However, proapoptotic protein Puma was lower in p53 knockdown cells but was induced by the AZD/Nutlin combination in both cell types. MDM2 induction by Nutlin-3a was

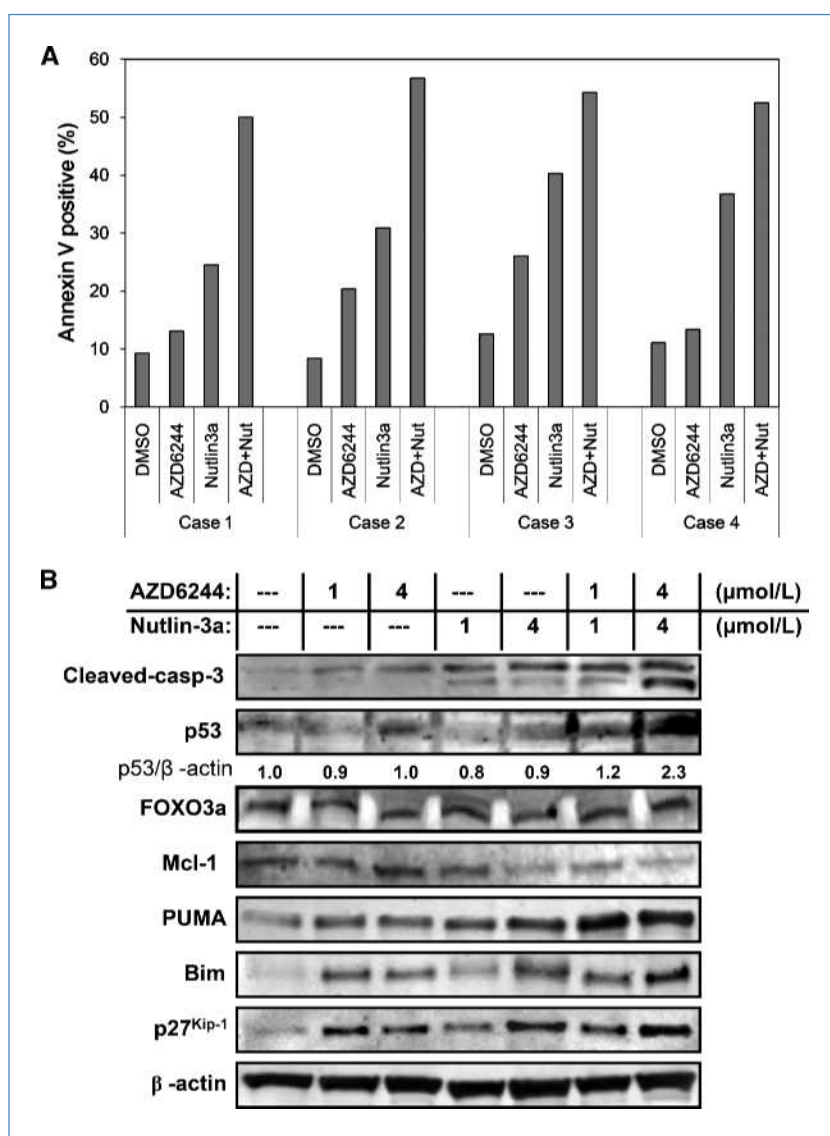


Figure 3. The effects of combined targeting of MEK/MDM2 signaling on AML patients *ex vivo*. A, peripheral blood and bone marrow blasts from patients with AML were treated with AZD6244 (4 $\mu\text{mol/L}$) and Nutlin-3a (4 $\mu\text{mol/L}$) for 24 h *ex vivo*, and apoptosis was determined as described in Materials and Methods. B, the expression of apoptosis-related proteins was analyzed by immunoblotting in sample 2. β -Actin was used as a loading control.

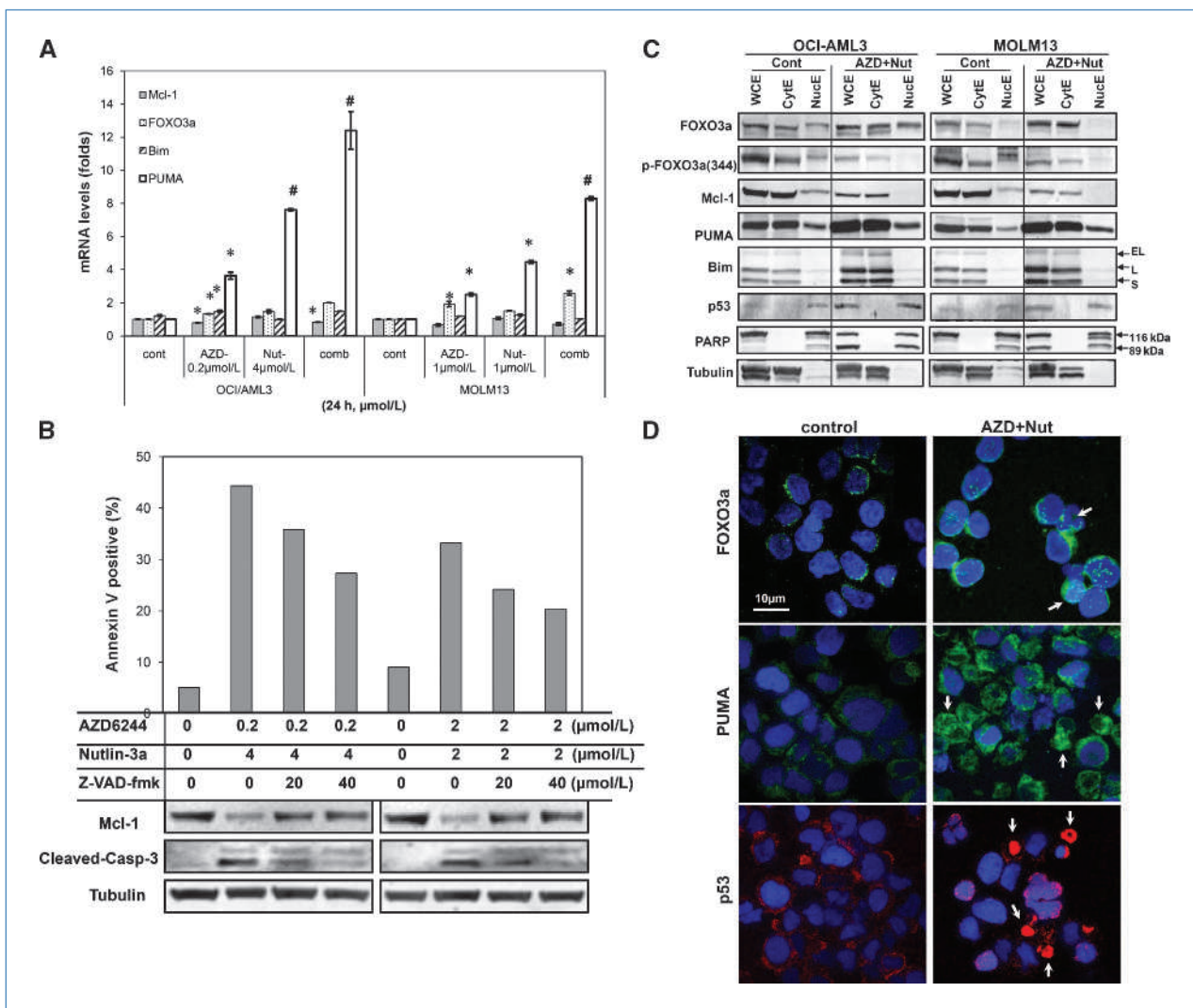


Figure 4. The effect of combined treatment with AZD6244 and Nutlin-3a on transactivation and location of apoptosis-related proteins in AML cells. A, OCI/AML3 and MOLM13 cells were treated for 24 h with AZD6244 plus Nutlin-3a (in 1:20 and 1:1 ratio, respectively, in OCI-AML3 and MOLM13 cells). DMSO only was used as a control (cont). The transcription levels of FOXO3a, Puma, Bim, and Mcl-1 were measured using real-time PCR. The results are presented as the mean changes in mRNA levels from duplicate experiments. Error bars correspond to 95% CIs. *, $P < 0.05$ and #, $P < 0.01$ versus control groups. B, Mcl-1 and cleaved caspase-3 protein levels were measured by Western blot, and cell apoptosis was measured by flow cytometry after 1 h of pretreatment with pan-caspase inhibitor (Z-VAD-fmk, R&D System) and additional 23 h of treatment of AZD6244/Nutlin-3a. C, the levels of the indicated proteins were determined by measuring the WCE, CytE, and NucE fractions. EL, L, and S indicate extralonal, long, and short splice variants of Bim proteins, respectively. Poly(ADP-ribose) polymerase (PARP) was used as loading control for the nuclear fraction, and tubulin was used as loading control for the cytoplasmic fraction. D, the subcellular distribution of FOXO3a, Puma, and p53 proteins was determined by immunofluorescence staining and visualized by confocal microscopy. The secondary antibodies to FOXO3a and Puma were conjugated with Alexa Fluor 488 (green), and the secondary anti-p53 antibody was conjugated with Alexa Fluor 594 (red). Nuclei were counterstained with 4',6-diamidino-2-phenylindole (blue). The arrows indicate apoptotic cells.

profound, as expected, in a p53-dependent fashion, but this induction was inhibited by AZD6244 (Fig. 2C).

Furthermore, effects of AZD6244 and/or Nutlin-3a treatment were investigated in four primary AML samples. The combination treatment enhanced apoptosis induction in both peripheral blood (samples 2–4) and bone marrow blasts (sample 1). The mean CI was 0.52 ± 0.01 (Fig. 3A). This was associated with upregulation of Puma and Bim and downregulation of Mcl-1, with little change in FOXO3a protein expression (Fig. 3B). Whereas samples 1 and 3 were derived from

AML patients harboring FLT3-ITD mutation, comparable increase in apoptosis was observed in all four samples tested.

Next, we further examined the mechanisms of changes in protein expression by determining mRNA levels of FOXO3a, Puma, Bim, and Mcl-1 in OCI/AML3 and MOLM13 cells by real-time PCR after AZD6244 and/or Nutlin-3a treatment. Results indicated that AZD6244, Nutlin-3a, or the combination minimally affected the mRNA expression levels of FOXO3a, Bim, and Mcl-1. However, AZD-6244, Nutlin-3a, and more so the combination enhanced mRNA levels of Puma (Fig. 4A).

The pan-caspase inhibitor Z-VAD-fmk reduced AZD6244/Nutlin-3a-induced apoptosis by suppressing caspase activation and concomitantly prevented the decrease in Mcl-1 levels, suggesting that Mcl-1 reduction was induced by caspase cleavage (Fig. 4B). Further investigation of the cellular location of these proteins in OCI/AML3 and MOLM13 cells showed that combination treatment increased total FOXO3a protein expression in whole-cell extract (WCE) and cytosolic extract (CytE), but less in the nuclear fraction. Likewise, phosphorylated FOXO3a (at Ser³⁴⁴ and Ser⁴²⁵) was decreased in WCE and CytE, but less in nuclear extract (NucE). The levels of Puma and Bim increased significantly in CytE and only moderately in NucE, whereas p53 protein increased in NucE (Fig. 4C). Immunofluorescence staining confirmed those expression patterns of FOXO3a, Puma, and p53 in OCI/AML3 cells; i.e., upregulation of FOXO3a and Puma protein levels occurred mainly in the cytoplasm, whereas p53 exhibited nuclear translocation after combination treatment with AZD6244 and

Nutlin-3a (Fig. 4D). The expression levels of Puma and p53 were impressively higher in cells undergoing apoptosis (Fig. 4D, arrows).

Knockdown of Puma and Bim rescues AML cells from apoptosis induced by AZD6244 and Nutlin-3a. Because blockade of ERK and MDM2 signaling upregulated protein levels of FOXO3a, Puma, and Bim, we next determined which proteins played a key role in combination-mediated apoptosis. The expression of FOXO3a, Puma, or Bim was knocked down using specific siRNAs in OCI/AML3 cells. Significant (>70%) suppression of the target protein levels was confirmed by immunoblotting (Fig. 5A, insert). OCI/AML3 cells transfected with mock siRNA became apoptotic (50.8 ± 1.9%) after 24 hours of combination treatment. However, Puma knockdown significantly diminished the apoptosis induced by combined AZD6244/Nutlin-3a treatment (to 22 ± 0.6%), and knockdown of Bim moderately decreased apoptosis (to 33 ± 1.6%). Only a minor decrease was observed in FOXO3a

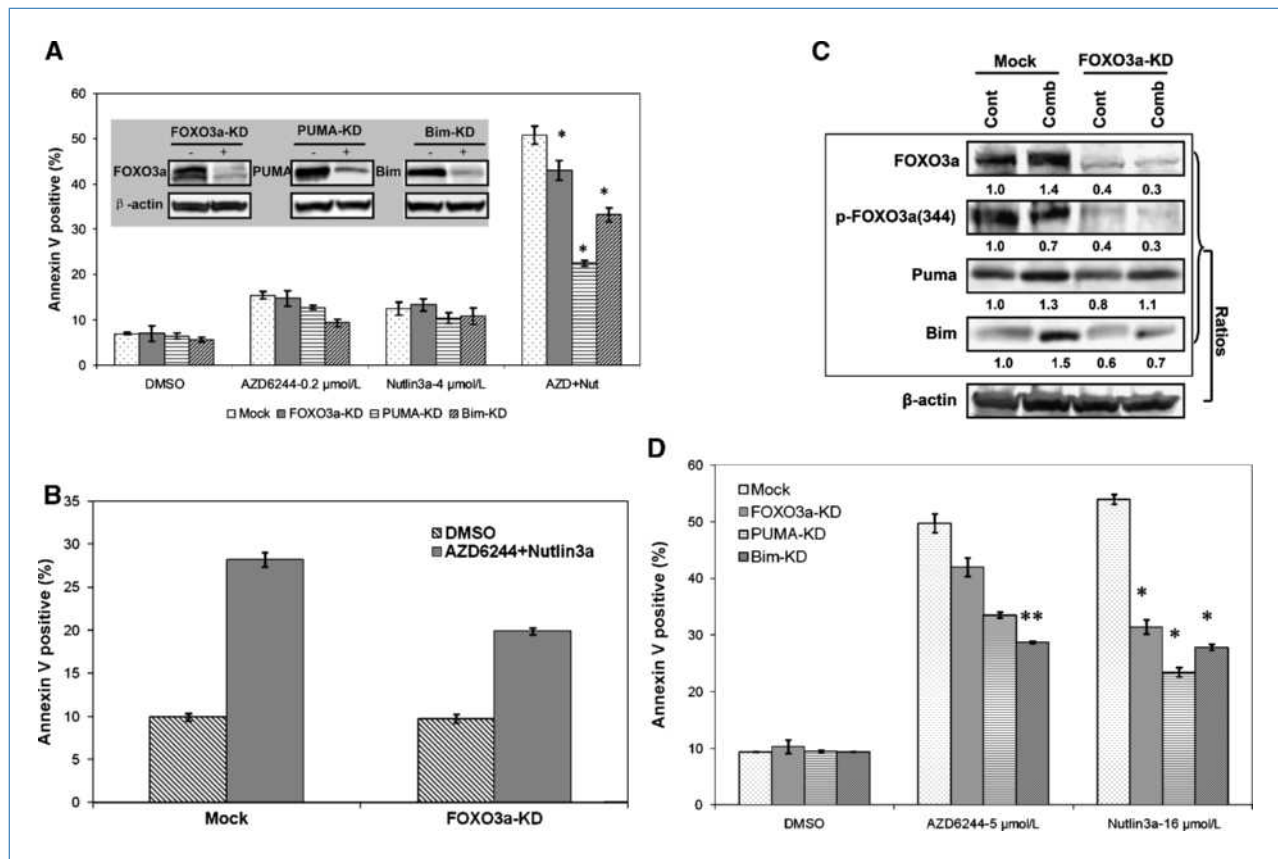


Figure 5. A, effects of knockdown of the indicated proteins on AZD6244- and/or Nutlin-3a-mediated AML cell apoptosis. OCI/AML3 cells were transiently transfected with FOXO3a, Puma and Bim siRNAs or mock control siRNA using Amaxa nucleofection. After 24 h, AZD6244 (0.2 μmol/L) and Nutlin-3a (4 μmol/L) or DMSO were added for additional 24 h, and the percentage of apoptotic (Annexin V-positive) cells was determined by flow cytometry. Data were generated from triplicate experiments. Insert, basal levels of FOXO3a, Puma, and Bim, which were determined by Western blot after 48 h of transfection. B, after transfection with FOXO3a or mock siRNA for 24 h, the OCI/AML3 cells were exposed to AZD6244 (1 μmol/L) and Nutlin-3a (12 μmol/L) or DMSO for additional 6 h. The percentage of apoptotic cells was measured by flow cytometry. C, the expression levels of the indicated proteins were measured by immunoblotting. Data were generated from duplicate experiments. D, OCI/AML3 cells were transfected with the indicated siRNAs for 24 h, followed by treatment with AZD6244 (5 μmol/L), Nutlin-3a (16 μmol/L), or DMSO for additional 24 h. The percentage of Annexin V-positive cells was determined by flow cytometry. Data represent triplicate experiments. *, $P < 0.01$; **, $P < 0.05$ versus mock control group.

knockdown relative to control cells (Fig. 5A). To reduce the potential nonspecific effects of FOXO3a knockdown, combination treatment was shortened to only 6 hours after transfection of cells with FOXO3a siRNA for 24 hours. Knockdown of FOXO3a partially diminished apoptosis induction (from $28 \pm 0.9\%$ to $20 \pm 0.4\%$) by combined AZD6244/Nutlin-3a treatment (Fig. 5B), and this was associated with partial inhibition of induction of Puma and Bim proteins (Fig. 5C). To further investigate the effects of knocking down these proteins on apoptosis induction by AZD6244 and Nutlin-3a alone, higher concentrations of the inhibitors were used, which would result in ~50% apoptosis in mock siRNA-transfected cells. The results showed that Nutlin-3a-mediated apoptosis was significantly abrogated in the cells with knockdown of FOXO3a, Puma, or Bim proteins. However, AZD6244-mediated apoptosis was most diminished in Bim knockdown cells and less so in Puma knockdown cells (Fig. 5D). These results suggested that Puma is a critical mediator of apoptosis induced by Nutlin-3a and by the Nutlin-3a/AZD6244 combination in p53 wild-type OCI/AML3 leukemia cells. In turn, Bim is likely a key regulator in AZD6244-induced apoptosis.

Discussion

The detailed mechanisms of growth inhibition caused by simultaneous inhibition of MEK/MDM2 signaling pathways remain undetermined. It is well established that inhibition of cell proliferation by MEK inhibitors is mediated by G₁ cell cycle arrest. In this study, we have shown synergistic p53-dependent inhibition of cell proliferation (BrdUrd incorporation) upon combined targeting of MEK/MDM2 signaling by AZD6244 and Nutlin-3a in leukemia cells. Progression through the cell cycle is executed through serial steps controlled by key checkpoint proteins. During early/mid G₁, cyclin D activates its associated CDKs (CDK4 and CDK6), promoting phosphorylation of retinoblastoma. In late G₁ phase, the cyclin E/CDK2 heterodimeric complex mediates further phosphorylation of retinoblastoma and subsequent release of E2F, which acts as a transcriptional activator by binding to sites on the promoters of genes essential for DNA synthesis (30). In turn, the "Cip/Kip" proteins p27^{Kip1} and p21^{Cip1} function as regulators of cell cycle progression at G₁ by directly inhibiting G₁ phase-related checkpoint proteins and arresting cells in G₁ phase. Notably, the combination treatment upregulated p53 and p27^{Kip1}, downregulated G₁ cell cycle checkpoint proteins cyclin E/cdk2 complex, cyclin D1/cdk4 complex, and cdc2, and suppressed phosphorylation of retinoblastoma. Growth inhibitory effects of combined MEK/MDM2 blockade were independent of p16^{INK4a}, one of the modulators of cyclin D1 expression (data not shown). In addition, p21 levels were modulated differently in OCI/AML3 and MOLM13 cells despite consistent growth inhibition observed in both cell types (Fig. 2A), indicating that p21 is not the key protein responsible for the observed cell cycle arrest. Further studies are needed to precisely map the convergence point of cell cycle regulation by these two agents.

The limited induction of apoptosis by suppressing MEK has been reported (21). Our present study showed that

AZD6244 at 0.2 nmol/L concentration for 24 hours induced only modest apoptosis but combined with Nutlin-3a significantly induced apoptosis in OCI/AML3 and MOLM13 cells, although suppression of phosphorylated ERK was almost at the same level (Fig. 2B). This finding further supports the fact that suppression of ERK activation might not be sufficient for apoptosis induction in AML, and optimized combination strategies need to be developed.

We have previously reported that the combination of MEK inhibitor PD98059 with MDM2 antagonist Nutlin-3a synergistically induced apoptosis in human OCI/AML3 cells. This was at least in part attributed to the ability of PD98059 to antagonize p53-mediated p21 induction, triggered by Nutlin-3a, which abrogates p21-mediated apoptotic resistance (31). However, in the present study using second generation of MEK inhibitor AZD6244 plus Nutlin-3a, modulation of p21 level did not parallel cell cycle arrest or apoptosis induction, and p21 levels in fact increased in MOLM13 cells after combination treatment (Fig. 2A). In turn, we observed upregulation of BH3-only proteins Puma and Bim and downregulation of antiapoptotic protein Mcl-1 associated with apoptosis induction (Fig. 3A). This was associated with p53-dependent suppression of FOXO3a phosphorylation at both Ser³⁴⁴ and Ser⁴²⁵ sites and upregulation of the total levels of FOXO3a, a known transcriptional activator of Puma, Bim, and p27^{Kip1} mRNA (32–34).

FOXO3a signaling has been reported to be modulated by phosphoinositide 3-kinase/AKT signaling pathway in response to growth factor stimulation via AKT-dependent phosphorylation of FOXO3a, leading to its degradation in the cytoplasm (35). FOXO3a also is nontranscriptionally regulated by E2F-1 as its direct downstream target during neuronal apoptosis (36), which is independent of p53 (37). However, in the present study, AZD6244 or Nutlin-3a did not affect AKT phosphorylation or E2F-1 levels (Fig. 2B), implying alternative mechanisms involved in the regulation of FOXO3a. As such, FOXO3a was recently shown to be degraded through MDM2-mediated ubiquitination following direct phosphorylation by ERK at several sites (Ser²⁹⁴, Ser³⁴⁴, and Ser⁴²⁵; ref. 38). In fact, our data showed that inhibition of phosphorylated ERK by targeting MEK/ERK signaling was associated with dephosphorylation of FOXO3a at Ser³⁴⁴ and further dephosphorylation at Ser³⁴⁴ and Ser⁴²⁵ by simultaneous targeting of MEK/MDM2 signaling. The latter might result from increased ubiquitination activity mediated by MDM2, which is likely induced via p53 in p53 wild-type cells. Interestingly, total FOXO3a level increased in p53 knockdown cells after either single-agent or combination treatment. We noted that basal expression of FOXO3a was also maintained at higher level in p53 knockdown cells compared with their parental p53 wild-type cells. Lower basal level of MDM2 negatively correlated to the higher FOXO3a level, suggesting that reduced degradation activation of MDM2 to FOXO3a protein may result in increasing of FOXO3a level. However, apoptosis induction in p53 knockdown cells were lower than that in p53 wild-type cells, and knocking down FOXO3a by shRNA only modestly reversed apoptosis induction. These suggest that FOXO3a itself is not the key mediator of apoptosis upon

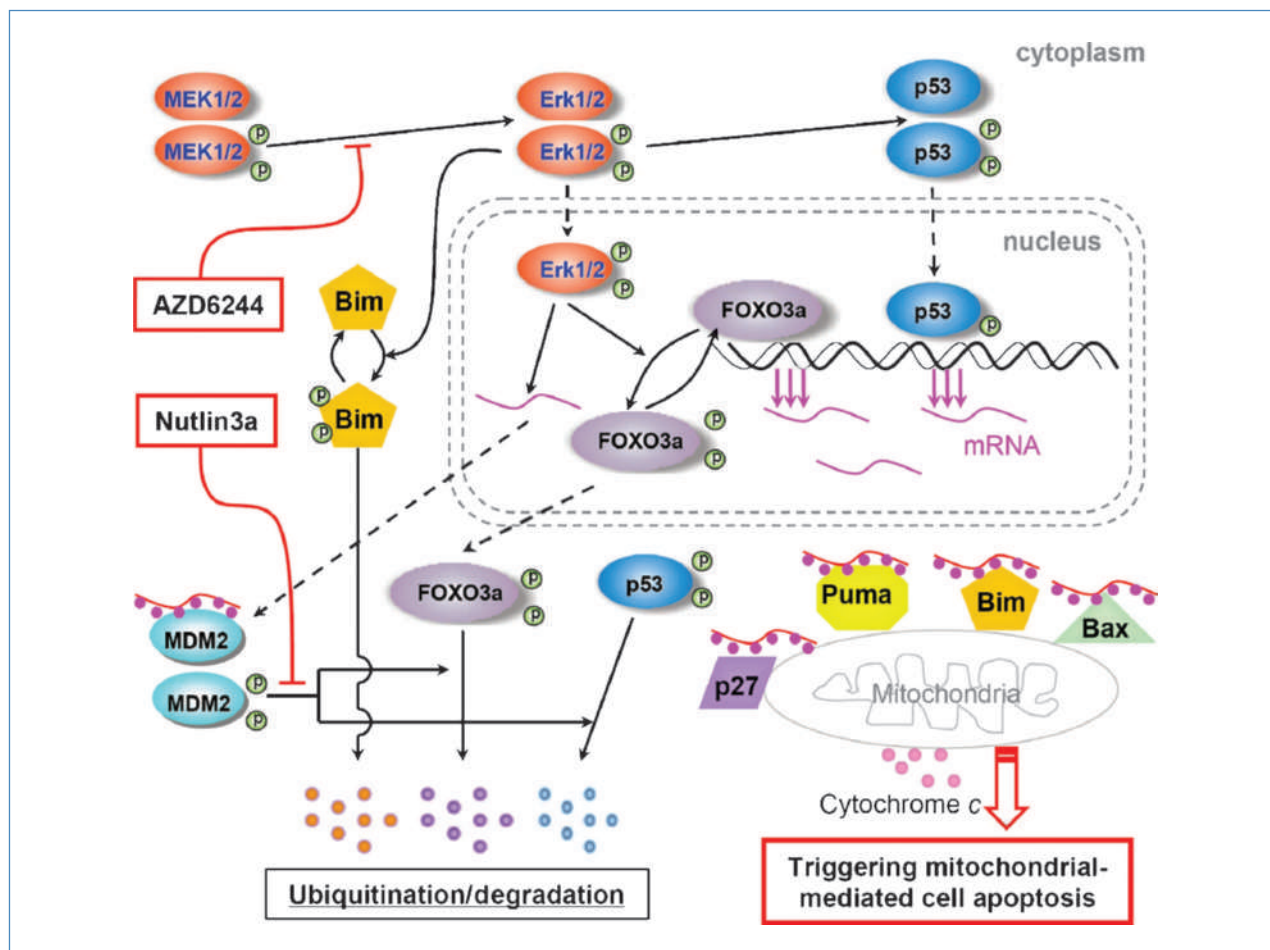


Figure 6. Mechanisms of synergistic apoptosis induction via combined blockade of MAPK and MDM2 signaling pathways in AML cells. FOXO3a and p53 are transcription factors that modulate levels of the proapoptotic proteins Puma, Bim, Bax, and p27. This schematic diagram illustrates an interaction of MEK/ERK signaling and an MDM2-p53 feedback loop and their interface with ubiquitination/degradation of FOXO3a and p53 proteins. FOXO3a and p53 are the main transcription factors regulating the levels of Puma, Bim, Bax, and p27 proteins (44–48). ERK activation triggers phosphorylation of FOXO3a at several sites (Ser²⁹⁴, Ser³⁴⁴, and Ser⁴²⁵; ref. 38) and promotes phosphorylation of Bim (49). MAPK signaling is further involved in maintaining the dynamic equilibrium of the MDM2-p53 feedback loop by modulating the phosphorylation level of p53 and the nuclear export of MDM2 mRNA (50, 51). In turn, MDM2 exerts regulation of FOXO3a and p53 levels by ubiquitination-mediated degradation (4, 38). Simultaneous blockade of MEK/ERK and MDM2 signaling contributes to the mitochondrial-mediated cell apoptosis by upregulating FOXO3a and p53 levels and transactivating Puma, Bim, and other proapoptotic proteins.

combined MEK/MDM2 blockade. Further studies are required to determine the regulation mechanism and precise role of FOXO3a in leukemic cell apoptosis.

Impressively, the transcription level of BH3-only protein Puma, which was originally identified as a p53-inducible gene (39), significantly increased (up to 12.4-fold and 8.3-fold in OCI/AML3 and MOLM13 cells, respectively) in wild-type p53 AML cells upon Nutlin or combined Nutlin/AZD treatment (Fig. 4A), indicating p53-dependent upregulation of this BH3-only protein. However, Puma also increased upon combined drug exposure in p53 knockdown cells, suggesting additional mechanisms of Puma upregulation. As such, FOXO3a has been reported to play a role in p53-independent Puma gene regulation (33). Most importantly, knockdown of Puma expression by shRNA dramatically reversed Nutlin-3a- and AZD6244/Nutlin-3a-induced cell apoptosis. Altogether, these

findings point out to the critical role of Puma in apoptosis induction upon combined MEK/MDM2 blockade, possibly by modulating other Bcl-2 family members, such as Bim, Mcl-1, and Bax.

The role of Bim in apoptosis induction of hematopoietic cells has been previously addressed in several experimental systems. It has been reported that inhibition of ERK1/2 activation is necessary and sufficient to promote substantial increase of Bim protein level by interfering ERK1/2-dependent degradation of Bim (40). Furthermore, blocking interaction of MDM2 and p53 may upregulate MDM2 level itself, resulting in Bim accumulation. In fact, our data showed that blocking either MEK or MDM2 upregulated Bim levels, and this effect was enhanced by the combined drugs treatment. No significant changes in mRNA Bim expression was noted, suggesting that the upregulation more likely results from interfering

with the protein degradation rather than activating its transcription. On the other hand, knockdown of Bim by shRNA only partially rescued AML cells from AZD/Nutlin-induced cell apoptosis, suggesting the contributory, but not central, role of Bim in the lethality of combined MEK/MDM2 blockade.

In addition, the effects of antiapoptotic Bcl-2 family member Mcl-1 in apoptosis induction has been reported, which presents as a complex of Bim/Mcl-1, Puma/Mcl-1, or Bax/Mcl-1 for maintaining and regulating normal hematopoietic homeostasis physiologically. When apoptotic signals are received, upregulated Puma and Bim can displace Mcl-1 from Bak leading to Bak oligomerization, and then Bim and Puma can interact with Bax, causing its insertion into outer mitochondrial membrane, oligomerization, and cytochrome *c* release. On the other hand, Mcl-1 protein itself can be regulated by transcription and/or E3 ubiquitination degradation (41). In addition, inhibition of Mcl-1 sensitized MEK inhibitor U0126-induced apoptosis in melanoma patients (42). Our present data showed that blocking either MEK or MDM2 led to downregulation of Mcl-1 and upregulation of Bax, and the modulation was synergized by the combined drug treatment, which was more significant in OCL/AML3 cells, which induced more apoptosis compared with MOLM13 cells. However, the decrease in Mcl-1 protein could be prevented by the pan-caspase inhibitor Z-VAD-fmk, which only slightly reduced apoptosis induction, suggesting that Mcl-1 might not be crucial in AZD6244/Nutlin-3a-induced cell death.

On the basis of these findings, we propose that the Bcl-2 family proteins Puma, Bim, Bax, and Mcl-1, rather than FOXO3a, are key contributors to the proapoptotic effects in combined blockade of the MAPK and MDM2 signaling pathways in p53 wild-type AML. In fact, Puma and Bim can be directly upregulated by p53 activation and ERK inhibition, respectively, and trigger mitochondrial-mediated apoptosis in AML cells by associating with other Bcl-2 family proteins, such as Bax and Mcl-1 (42, 43). That may explain why knockdown of FOXO3a only is insufficient to abrogate apoptosis mediated by combined treatment with AZD6244 and Nutlin-3a. However, knockdown of Puma and Bim resulted in protection of cells from AZD/Nutlin-induced cell death. This was further substantiated by our confocal microscopy data, showing dramatic upregulation of Puma but not of FOXO3a in early-stage apoptotic cells. Puma knockdown resulted in protection from apoptosis induction by high concentrations of Nutlin-3a,

whereas Bim knockdown significantly diminished the proapoptotic effects of high concentrations of AZD6244. Taken together, these findings indicate that the level of Puma is regulated primarily via Mdm2/p53 axis, whereas Bim protein expression depends on MAPK activation status. FOXO3a facilitated the upregulation of Puma and Bim expression via either transcription or degradation.

In summary, our results show that the small molecule MEK1/2 inhibitor AZD6244 has a profound cytostatic effect on AML cells with constitutive activation of MEK/ERK signaling. In turn, cytotoxic effects of MEK inhibition are synergistically induced by targeting MDM2-p53 axis with Nutlin-3a. Mechanistically, Puma and Bim were identified as critical mediators of apoptosis induced by simultaneous blockade of MEK and MDM2 signaling, which is partially mediated by transcriptional activation of FOXO3a. These pleiotropic effects are summarized in a model illustrated in Fig. 6. Our findings for the first time identify Puma and Bim as factors in apoptosis induced by combined AZD6244 and Nutlin-3a treatment in AML cell lines and primary AML blasts. Altogether, these results strongly suggest that combinatorial targeting of MEK and MDM2 with AZD6244 and Nutlin-3a has potential as a novel mechanism-based therapeutic strategy for AML.

Disclosure of Potential Conflicts of Interest

The study sponsor had no role in the design of the study; the collection, analysis, or interpretation of the data; the writing of the manuscript; or the decision to submit the manuscript for publication. No potential conflicts of interest were disclosed.

Acknowledgments

We thank Wenjing Chen for the valuable assistance in the collection of patients' clinical information and Karen Phillips for editorial assistance.

Grant Support

NIH grants CA55164, CA016672, and CA100632 (M. Andreeff); Leukemia Specialized Programs of Research Excellence Career Development Award CA100632 (W. Zhang); and AstraZeneca (M. Andreeff).

The costs of publication of this article were defrayed in part by the payment of page charges. This article must therefore be hereby marked *advertisement* in accordance with 18 U.S.C. Section 1734 solely to indicate this fact.

Received 03/09/2009; revised 12/10/2009; accepted 12/29/2009; published OnlineFirst 03/09/2010.

References

- Ricciardi MR, McQueen T, Chism D, et al. Quantitative single cell determination of ERK phosphorylation and regulation in relapsed and refractory primary acute myeloid leukemia. *Leukemia* 2005;19:1543–9.
- Kornblau SM, Womble M, Qiu YH, et al. Simultaneous activation of multiple signal transduction pathways confers poor prognosis in acute myelogenous leukemia. *Blood* 2006;108:2358–65.
- Seliger B, Papadileris S, Vogel D, et al. Analysis of the p53 and MDM2 gene in acute myeloid leukemia. *Eur J Haematol* 1996;57:230–40.
- Haupt Y, Maya R, Kazaz A, Oren M. Mdm2 promotes the rapid degradation of p53. *Nature* 1997;387:296–9.
- Vogelstein B, Kinzler KW. p53 function and dysfunction. *Cell* 1992;70:523–6.
- McMurray HR, Sampson ER, Compitello G, et al. Synergistic response to oncogenic mutations defines gene class critical to cancer phenotype. *Nature* 2008;453:1112–6.
- Blalock WL, Moyer PW, Chang F, et al. Combined effects of aberrant MEK1 activity and BCL2 overexpression on relieving the cytokine dependency of human and murine hematopoietic cells. *Leukemia* 2000;14:1080–96.
- Moyer PW, Blalock WL, Hoyle PE, et al. Synergy between Raf and BCL2 in abrogating the cytokine dependency of hematopoietic cells. *Leukemia* 2000;14:1060–79.
- Kerr AH, James JA, Smith MA, Willson C, Court EL, Smith JG. An investigation of the MEK/ERK inhibitor U0126 in acute myeloid leukemia. *Ann N Y Acad Sci* 2003;1010:86–9.

10. Milella M, Konopleva M, Precupanu CM, et al. MEK blockade converts AML differentiating response to retinoids into extensive apoptosis. *Blood* 2007;109:2121–9.
11. Lunghi P, Tabilio A, Dall'Aglio PP, et al. Downmodulation of ERK activity inhibits the proliferation and induces the apoptosis of primary acute myelogenous leukemia blasts. *Leukemia* 2003;17:1783–93.
12. Milella M, Kornblau SM, Estrov Z, et al. Therapeutic targeting of the MEK/MAPK signal transduction module in acute myeloid leukemia. *J Clin Invest* 2001;108:851–9.
13. Zhang W, Konopleva M, Ruvolo VR, et al. Sorafenib induces apoptosis of AML cells via Bim-mediated activation of the intrinsic apoptotic pathway. *Leukemia* 2008;22:808–18.
14. Huynh H, Soo KC, Chow PK, Tran E. Targeted inhibition of the extracellular signal-regulated kinase kinase pathway with AZD6244 (ARRY-142886) in the treatment of hepatocellular carcinoma. *Mol Cancer Ther* 2007;6:138–46.
15. Tai YT, Fulciniti M, Hideshima T, et al. Targeting MEK induces myeloma-cell cytotoxicity and inhibits osteoclastogenesis. *Blood* 2007;110:1656–63.
16. Davies BR, Logie A, McKay JS, et al. AZD6244 (ARRY-142886), a potent inhibitor of mitogen-activated protein kinase/extracellular signal-regulated kinase kinase 1/2 kinases: mechanism of action *in vivo*, pharmacokinetic/pharmacodynamic relationship, and potential for combination in preclinical models. *Mol Cancer Ther* 2007;6:2209–19.
17. Ball DW, Jin N, Rosen DM, et al. Selective growth inhibition in BRAF mutant thyroid cancer by the mitogen-activated protein kinase kinase 1/2 inhibitor AZD6244. *J Clin Endocrinol Metab* 2007;92:4712–8.
18. Yeh TC, Marsh V, Bernat BA, et al. Biological characterization of ARRY-142886 (AZD6244), a potent, highly selective mitogen-activated protein kinase kinase 1/2 inhibitor. *Clin Cancer Res* 2007;13:1576–83.
19. Haass NK, Sproesser K, Nguyen TK, et al. The mitogen-activated protein/extracellular signal-regulated kinase kinase inhibitor AZD6244 (ARRY-142886) induces growth arrest in melanoma cells and tumor regression when combined with docetaxel. *Clin Cancer Res* 2008;14:230–9.
20. Zhang W, Konopleva M, Schober W, McQueen T, Andreeff M. MEK Inhibitor AZD6244 (ARRY-142886) Induces Cell Growth Arrest and Synergizes with Nutlin-3a-mediated Cell Death by Up-regulating p53 and PUMA Levels in AML (ASH Abstract). *Blood* 2008;110:201a.
21. Milella M, Precupanu CM, Gregorj C, et al. Beyond single pathway inhibition: MEK inhibitors as a platform for the development of pharmacological combinations with synergistic anti-leukemic effects. *Curr Pharm Des* 2005;11:2779–95.
22. Kojima K, Konopleva M, Samudio IJ, et al. MDM2 antagonists induce p53-dependent apoptosis in AML: implications for leukemia therapy. *Blood* 2005;106:3150–9.
23. Kojima K, Konopleva M, Samudio IJ, Ruvolo V, Andreeff M. Mitogen-activated protein kinase kinase inhibition enhances nuclear pro-apoptotic function of p53 in acute myelogenous leukemia cells. *Cancer Res* 2007;67:3210–9.
24. Carter BZ, Mak DH, Schober WD, et al. Triptolide sensitizes AML cells to TRAIL-induced apoptosis via decrease of XIAP and p53-mediated increase of DR5. *Blood* 2008;111:3742–50.
25. Clodi K, Kliche K-O, Zhao S, et al. Cell-surface exposure of phosphatidylserine correlates with the stage of fludarabine-induced apoptosis in chronic lymphocytic leukemia (CLL) and expression of apoptosis-regulating genes. *Cytometry* 2000;40:19–25.
26. Zhang W, McQueen T, Schober W, Rassidakis G, Andreeff M, Konopleva M. Leukotriene B4 receptor inhibitor LY293111 induces cell cycle arrest and apoptosis in human anaplastic large-cell lymphoma cells via JNK phosphorylation. *Leukemia* 2005;19:1977–84.
27. Konopleva M, Zhang W, Shi YX, et al. Synthetic triterpenoid 2-cyano-3,12-dioxooleana-1,9-dien-28-oic acid induces growth arrest in HER2-overexpressing breast cancer cells. *Mol Cancer Ther* 2006;5:317–28.
28. Zhao L, Wientjes MG, Au JL. Evaluation of combination chemotherapy: integration of nonlinear regression, curve shift, isobologram, and combination index analyses. *Clin Cancer Res* 2004;10:7994–8004.
29. Chou TC, Talalay P. Quantitative analysis of dose-effect relationships: the combined effects of multiple drugs or enzyme inhibitors. *Adv Enzyme Regul* 1984;22:27–55.
30. Johnson DG, Schneider-Broussard R. Role of E2F in cell cycle control and cancer. *Front Biosci* 1998;3:d447–8.
31. Gartel AL, Tyner AL. The role of the cyclin-dependent kinase inhibitor p21 in apoptosis. *Mol Cancer Ther* 2002;1:639–49.
32. Gilley J, Coffey PJ, Ham J. FOXO transcription factors directly activate bim gene expression and promote apoptosis in sympathetic neurons. *J Cell Biol* 2003;162:613–22.
33. You H, Pellegrini M, Tsuchihara K, et al. FOXO3a-dependent regulation of Puma in response to cytokine/growth factor withdrawal. *J Exp Med* 2006;203:1657–63.
34. Dong S, Kang S, Lonial S, Khoury HJ, Viallet J, Chen J. Targeting 14–3–3 sensitizes native and mutant BCR-ABL to inhibition with U0126, rapamycin and Bcl-2 inhibitor GX15-070. *Leukemia* 2008;22:572–7.
35. Brunet A, Bonni A, Zigmond MJ, et al. Akt promotes cell survival by phosphorylating and inhibiting a Forkhead transcription factor. *Cell* 1999;96:857–68.
36. Nowak K, Killmer K, Gessner C, Lutz W. E2F-1 regulates expression of FOXO1 and FOXO3a. *Biochim Biophys Acta* 2007;1769:244–52.
37. Giovanni A, Keramaris E, Morris EJ, et al. E2F1 mediates death of B-amyloid-treated cortical neurons in a manner independent of p53 and dependent on Bax and caspase 3. *J Biol Chem* 2000;275:11553–60.
38. Yang JY, Zong CS, Xia W, et al. ERK promotes tumorigenesis by inhibiting FOXO3a via MDM2-mediated degradation. *Nat Cell Biol* 2008;10:138–48.
39. Yu J, Zhang L, Hwang PM, Kinzler KW, Vogelstein B. PUMA induces the rapid apoptosis of colorectal cancer cells. *Mol Cell* 2001;7:673–82.
40. Ley R, Balmanno K, Hadfield K, Weston C, Cook SJ. Activation of the ERK1/2 signaling pathway promotes phosphorylation and proteasome-dependent degradation of the BH3-only protein, Bim. *J Biol Chem* 2003;278:18811–6.
41. Akgul C. Mcl-1 is a potential therapeutic target in multiple types of cancer. *Cell Mol Life Sci* 2009;66:1326–36.
42. Wang YF, Jiang CC, Kiejda KA, Gillespie S, Zhang XD, Hersey P. Apoptosis induction in human melanoma cells by inhibition of MEK is caspase-independent and mediated by the Bcl-2 family members PUMA, Bim, and Mcl-1. *Clin Cancer Res* 2007;13:4934–42.
43. Michalak EM, Villunger A, Adams JM, Strasser A. In several cell types tumour suppressor p53 induces apoptosis largely via Puma but Noxa can contribute. *Cell Death Differ* 2008;15:1019–29.
44. Tran H, Brunet A, Griffith EC, Greenberg ME. The many forks in FOXO's road. *Sci STKE* 2003;2003:RE5.
45. Dijkers PF, Medema RH, Pals C, et al. Forkhead transcription factor FKHR-L1 modulates cytokine-dependent transcriptional regulation of p27(KIP1). *Mol Cell Biol* 2000;20:9138–48.
46. Dijkers PF, Medema RH, Lammers JW, Koenderman L, Coffey PJ. Expression of the pro-apoptotic Bcl-2 family member Bim is regulated by the forkhead transcription factor FKHR-L1. *Curr Biol* 2000;10:1201–4.
47. Vousden KH. Apoptosis. p53 and PUMA: a deadly duo. *Science* 2005;309:1685–6.
48. Meulmeester E, Jochemsen AG. p53: a guide to apoptosis. *Curr Cancer Drug Targets* 2008;8:87–97.
49. Weston CR, Balmanno K, Chalmers C, et al. Activation of ERK1/2 by δ Raf-1:ER* represses Bim expression independently of the JNK or PI3K pathways. *Oncogene* 2003;22:1281–93.
50. Milne DM, Campbell DG, Caudwell FB, Meek DW. Phosphorylation of the tumor suppressor protein p53 by mitogen-activated protein kinases. *J Biol Chem* 1994;269:9253–60.
51. Phelps M, Phillips A, Darley M, Blaydes JP. MEK-ERK signaling controls Hdm2 oncoprotein expression by regulating hdm2 mRNA export to the cytoplasm. *J Biol Chem* 2005;280:16651–8.